High Energy Resummation at Hadronic Colliders

Jack J. Medley

A thesis submitted in fulfilment of the requirements
for the degree of Doctor of Philosophy
to the
University of Edinburgh
March 2016

Abstract

Abstract abstract.

Declaration

Except where otherwise stated, the research undertaken in this thesis was the unaided work of the author. Where the work was done in collaboration with others, a significant contribution was made by the author.

J. Medley
March 2016

Acknowledgements

Cheers guys!

Contents

List of Figures

List of Tables

Chapter 1

Introduction

1.1 A Little History

The current 'Standard Model' of particle physics was completed in June 2012 with the announcement of the Higgs boson by the ATLAS collaboration. This discovery with the final piece needed to complete the picture developed over the course of the past century beginning with the discovery of the electron in 1897. The Standard Model is a gauge quantum field theory describing three of the four observed fundamental forces - with the inclusion of gravity remaining elusive. The local gauge structure is given by:

$$SU(3) \times SU(2) \times U(1), \tag{1.1}$$

where the $SU(3)$ describes the strong nuclear force (Quantum Chromodynamics or QCD), while the $SU(2)_L \times U(1)$ describes the electroweak (EW) sector.
The fundamental particle content can be broken down in to the following three catagories:

- Fermions: These spin-1/2 particles obey the spin-statistics theorem and comprise all the known visible matter in the universe. Comprising three so-called 'generations' fermions can be further subdivided in to quarks and leptons. Both quarks and leptons carry fractional electromagnetic charge but only quarks are charged under the strong $SU(3)$ group.

- Gauge bosons: These spin-1 excitations arise from the quantisation of the above gauge fields and mediate the three forces detailed above. The gauge

bosons of the strong and electromagnetic sectors are massless while the electroweak bosons acquire mass through famous Higgs mechanism.

- The Higgs boson: The Higgs boson is seen as the result of the spontaneous symmetry breaking of a continuous symmetry. This is a gauge-invariant way to give mass to fermions and vector bosons in the standard model which was crutial since such states had long been observed at experiments.

1.2 Thesis Outline

The aim of this thesis is to detail the importance of a certain class of perurbatibely high-order terms in events with QCD radiation in the final state. In particular corrections to parton-parton collisions with a Z/γ^* electroweak boson in the final state will be considered.
Firstly, in Chapter 2 I will introduce quantum chromodynamics, the theory of the strong sector in the standard model, and detail how we might use this to calculate physical observables (such as cross-sections and differential distributions) at hadron colliders such as the Large Hadron Collider. I will discuss how these observables fall prey to divergences in QCD-like quantum field theoreies with massless states and mention briefly how they may be dealt with. I will then describe how the compuationally expensive integrals derived may be efficiently evaluated using Monte-Carlo coupled with variance reduction techniques such as importance sampling.
In Chapter **??** the details of QCD in the 'High Energy' limit are discussed. We will see how, in this limit, the traditional fixed-order perturbative view of scattering cross-sections fades as another subset of terms, namely the Leading Logarithmic contributions, become more important.

Chapter 2

QCD at hadronic colliders

2.1 The QCD Lagrangian

The Lagrangian for QCD is more complicated than the one previously seen for QED. This is in part due to us having to sum over different representations of the generating group, $SU(3)$, but mainly because the fields no longer commute with one another (they are non-Abelian in nature) and this leads to gauge boson self-interactions. The full Lagrangian is as follows [**?**] [1]:

$$\mathcal{L}^{QCD} = \overline{\psi}^i \left(i \not{D}^{ij} - m\delta^{ij} \right) \psi^j - \frac{1}{4} F^a_{\mu\nu} F^{a\mu\nu} - \frac{1}{2\xi} (\partial^\mu A^a_\mu)^2 + (\partial^\mu \chi^{a*}) \mathcal{D}^{ab}_\mu \chi^b. \quad (2.1a)$$

$$D^{ij}_\mu = \delta^{ij} \partial_\mu - i g_s (T^c)^{ij} A^c_\mu. \quad (2.1b)$$

$$\mathcal{D}^{ab}_\mu = \delta^{ab} \partial_\mu - g_s f^{abc} A^c_\mu. \quad (2.1c)$$

where the indices i, j run from 1 to 3, the indices a, b, c run from 1 to 8, D_μ is the covariant derivative in the fundamental representation, $\mathcal{D}_\mu$ is the covariant derivative in the adjoint representation, T^a are the generating matrices and finally $f^{abc} = i(T^a_{adj})^{bc}$. The χ fields are the 'ghost' excitations and their origin will be explained in section 3.1.

In analogy to section (2) we begin by decomposing equation (12) into a free Lagrangian and an interacting Lagrangian as follows:

[1] With the bare quantity subscripts supressed

$$\mathcal{L}_0^{QCD} = \overline{\psi}^i \left(i\partial\!\!\!/ - m\right)\psi^i - \frac{1}{4}\partial_{[\mu}A^a_{\nu]}\partial^{[\mu}A^{\nu]a} - \frac{1}{2\xi}(\partial^\mu A^a_\mu)(\partial^\nu A^a_\nu) + (\partial^\mu \chi^{a*})(\partial_\mu \chi^a), \tag{2.2}$$

$$\mathcal{L}_I^{QCD} = g_s\overline{\psi}^i T^a_{ij}\gamma^\mu\psi^j - \frac{g_s}{2}f^{abc}\partial_{[\mu}A^a_{\nu]}A^{b\mu}A^{c\nu} - \frac{g_s^2}{4}f^{abe}f^{cde}A^a_\mu A^b_\nu A^{c\mu}A^{d\nu} - g_s f^{abc}\partial^\mu\chi^{a*}\chi^b A^c_\mu. \tag{2.3}$$

By calculating the QCD partition function and acting with the appropriate derivatives we can find the fermion propagator and the ghost propagator, repectively:

$$\langle 0|\psi_i(x)\psi_j(y)|0\rangle = S_F(x-y) = \int \frac{d^4k}{(2\pi)^4}e^{-ik\cdot(x-y)}\delta_{ij}\frac{i}{k\!\!\!/ - m + i\epsilon}, \tag{2.4}$$

$$\langle 0|\chi_a(x)\chi_b(y)|0\rangle = H_F(x-y) = \int \frac{d^4k}{(2\pi)^4}e^{-ik\cdot(x-y)}\delta_{ab}\frac{i}{k^2 + i\epsilon}. \tag{2.5}$$

and we can read off the various QCD vertex factors directly from the interaction Lagrangian.

2.1.1 The Faddeev-Popov Procedure for NAGTs

All that remains to be done is to evaluate the gluon propagator. As in QED when trying to compute the propagator of a massless gauge boson we can use the work of Faddeev and Popov. The functional integral we want to evaluate is in the form:

$$\int DA e^{-\frac{i}{4}\int d^4x F^a_{\mu\nu}F^{a\mu\nu}}. \tag{2.6}$$

Where $DA = \prod_x \prod_{a,\mu} dA^a_\mu$. As briefly outlined above we would like to perform a functional integration over all possible gauge choices and then pick out the subset of gauges we are interested in by enforcing the gauge condition $G(A) = 0$ to eliminate overcounting. This constraint may be written as [**?**]:

$$\int D\alpha(x)\delta(G(A^\alpha))Det\left(\frac{\delta G(A^\alpha)}{\delta\alpha(x)}\right) = 1. \tag{2.7}$$

Where $A^\alpha_\mu = A_\mu - \frac{1}{g_s}\partial_\mu\alpha(x)$. Making a gauge transformation ($A_\mu \to A^\alpha_\mu$) and

inserting equation (18):

$$\int DAe^{-\frac{i}{4}\int d^4F^a_{\mu\nu}F^{a\mu\nu}} = \int DA \int D\alpha(x)\delta(G(A^\alpha))Det\left(\frac{\delta G(A^\alpha)}{\delta\alpha(x)}\right)e^{-\frac{i}{4}\int d^4F^a_{\mu\nu}F^{a\mu\nu}}, \tag{2.8a}$$

$$= \int D\alpha(x)\int DA\delta(G(A^\alpha))Det\left(\frac{\delta G(A^\alpha)}{\delta\alpha(x)}\right)e^{-\frac{i}{4}\int d^4F^a_{\mu\nu}F^{a\mu\nu}}. \tag{2.8b}$$

We are free to change the functional integration variable to A^α_μ since everything is gauge invariant leading to an integrand which *only* depends on A^α_μ. We can therefore simply relabel back to A_μ:

$$= \left(\int D\alpha(x)\right)\int DA\delta(G(A))Det\left(\frac{\delta G(A)}{\delta\alpha(x)}\right)e^{-\frac{i}{4}\int d^4F^a_{\mu\nu}F^{a\mu\nu}}. \tag{2.9}$$

The functional integration can now just be factored out as a constant and we can choose the function $G(A)$ as a generalisation of the Lorentz gauge: $G(A) = \partial^\mu A^a_\mu - \omega^a$. This choice leads us to the correct gluon propagator - along with our free parameter, ξ:

$$\langle 0|A_a(x)A_b(y)|0\rangle = G^{\mu\nu}_F(x-y) = \int \frac{d^4x}{(2\pi)^4}e^{-ik\cdot(x-y)}\delta_{ab}\frac{-i}{k^2+i\epsilon}\left(g^{\mu\nu} - (1-\xi)\frac{k^\mu k^\nu}{k^2}\right). \tag{2.10}$$

but because the QCD gauge transformation is more involved than the QED eqivalent the determinant term still depends on A_μ:

$$Det\left(\frac{\delta G(A)}{\delta\alpha(x)}\right) = Det\left(\frac{\partial_\mu D^\mu}{g_s}\right). \tag{2.11}$$

We can however simply invent another type of field and choose to write out determinant as

$$Det\left(\frac{\delta G(A)}{\delta\alpha(x)}\right) = \int D\chi D\overline{\chi}e^{i\int d^4x\overline{\chi}(-\partial_\mu D_\mu)\chi}. \tag{2.12}$$

These non-physical modes are called the Faddeev-Popov ghosts/antighosts and are a consequence of enforcing gauge invariance - they are represented by the final term in equation (12a).

2.1.2 Renormalising the QCD Lagrangian

Similarly to QED we anticipate divergent quantities in our calculations above tree level and so we introduce counterterms into our Lagrangian. Similarly to equation (4) we have the following relations:

$$\psi_0 = Z_\psi^{\frac{1}{2}}\psi, \qquad A_0^a = Z_A^{\frac{1}{2}}A^a, \qquad \chi_0^a = Z_\chi^{\frac{1}{2}}\chi^a, \tag{2.13a}$$

$$m_0 = Z_m m, \qquad g_{s0} = Z_s g_s, \qquad \xi_0 = Z_\xi \xi. \tag{2.13b}$$

Inserting these into equations (13) and (14) and rearranging so that we have $\mathcal{L}^{\mathcal{QCD}} = \mathcal{L}_0 + \mathcal{L}_{ct}$ where $\mathcal{L}_0$ is as definied in equation (13) and the counterterm Lagrangian is:

$$\begin{aligned}\mathcal{L}_{ct} = &-(Z_A - 1)\frac{1}{4}(F_{\mu\nu}^a)^2 + (Z_\chi - 1)i(\partial^\mu\chi^a)(\partial_\mu\chi^a) + (Z_\psi - 1)\overline{\psi^i}(i\not{\partial} - m)\psi^i - Z_\psi(Z_m - 1)m\overline{\psi^i}\psi \\ &-(Z_s Z_A^{\frac{3}{2}} - 1)\frac{1}{2}g_s f^{abc}\partial_{[\mu}A_{\nu]}^a A^{b\mu}A^{c\nu} - (Z_s^2 Z_A^2 - 1)\frac{1}{4}g_s^2 f^{abe}f^{cde}A_\mu^a A_\nu^b A^{c\mu}A^{d\nu} - \dots \\ &-(Z_s Z_\chi Z_A^{\frac{1}{2}} - 1)ig_s f^{abc}(\partial^\mu\chi^a)\chi^b A_\mu^c + (Z_s Z_\psi Z_A^{\frac{1}{2}} - 1)g_s\overline{\psi}^i T_{ij}^a\gamma^\mu\psi^j A_\mu^a.\end{aligned} \tag{2.14}$$

2.2 Factorisation at Hadronic Colliders

2.3 A brief look at divergences and regularisation

2.4 Perturbative QCD and Resummation

2.4.1 Expansions in the strong coupling constant

2.4.2 An Example Fixed-Order Calculation

2.4.3 Limitations of Fixed-Order Schemes

2.4.4 Resumming Higher-Order Corrections

2.5 Spinor-Helicity Notation

Chapter 3

Monte Carlo Techniques

3.1 One Dimensional Monte Carlo

3.2 Higher Dimensional Monte Carlo

3.3 Variation Reduction Techniques

Chapter 4

High Energy QCD

4.1 The High Energy Limit of $2 \to 2$ QCD scattering

4.1.1 Mandelstam Variables in the High Energy Limit

The $2 \to 2$ QCD scattering amplitudes can be expressed in terms of the well-known Mandestam variables s, t and u. Which, in terms of the momenta in the process, are given by:

$$s = (p_1 + p_2)^2 \tag{4.1a}$$

$$t = (p_1 - p_2)^2 \tag{4.1b}$$

$$u = (p_2 - p_3)^3 \tag{4.1c}$$

When working in the high energy limit it is convenient to re-express these in terms of the perpendicular momentum of the outgoing partons, $p_\perp$, and the difference in rapidity between the two final state partons, δy:

$$s = 4p_\perp^2 \cosh^2 \frac{\Delta y}{2} \tag{4.2a}$$

$$t = -2p_\perp^2 \cosh \frac{\Delta y}{2} e^{-\frac{\Delta y}{2}} \tag{4.2b}$$

$$u = -2p_\perp^2 \cosh \frac{\Delta y}{2} e^{\frac{\Delta y}{2}} \tag{4.2c}$$

In the limit of hard jets well separated in rapidity these can be approximated to give

$$s \approx p_\perp^2 e^{\Delta y} \tag{4.3a}$$

$$t \approx -p_\perp^2 \tag{4.3b}$$

$$u \approx -p_\perp^2 e^{\Delta y} \tag{4.3c}$$

From equation (above) it is clear that the 'hard, wide-angle jet' limit is equivalent to the High Energy limit since:

$$\Delta y \approx \ln\left(\frac{s}{-t}\right) \tag{4.4}$$

4.1.2 HE limit of the three-gluon vertex

The three gluon vertex shown in figure (X) has the following Feynman rule:

$$g_s f^{abc}\left((p_1+p_3)^\nu g^{\mu_1\mu_3} + (q-p_3)^{\mu_1} g^{\mu_3\nu} - (q+p_1)^{\mu_3} g^{\mu_1\nu}\right) \tag{4.5}$$

In the high energy limit the emitted gluon with momenta q is much softer that the emitting gluon with momenta p_1 i.e. $p_1^\mu \gg q^\mu \ \forall\mu$ and therefore $p_1 \sim p_3$ - using this we can approximate the vertex by

$$\approx g_s f^{abc}\left(2p_1^\nu g^{\mu_1\mu_3} + p_3^{\mu_1} g^{\mu_3\nu} - p_3^{\mu_3} g^{\mu_1\nu}\right) \tag{4.6}$$

Furthermore, since the hard gluons in a high energy process are external they must satisfy the Ward identities; $\epsilon_1 \cdot p_1 = \epsilon_3 \cdot p_3 = 0$. Hence, the vertex can be expressed simply as:

$$\approx 2g_s f^{abc} p_1^\nu g^{\mu_1\mu_3} \tag{4.7}$$

4.1.3 At Leading Order in α_s

Talk through the limit of $2 \to 2$ scattering of gluons. Introduce mandelstam variables, show the equivalence of large delta y and large s.

4.1.4 At Next-to-Leading Order in α_s

Calculate the NLO calcuations to the 2j ME and show that there explicitly is a delta y (large log) enhancement.

4.1.5 High Energy Jets 'Currents'

4.1.6 Effective Vertices For Real Emissions

4.2 High Energy Jets

4.2.1 The Multi-Regge Kinematic limit of QCD amplitudes

4.2.2 HEJ currents

Pure Jets

4.2.3 Logarithms in HEJ observables

Here you should take a $2 \to n$ ME, apply the HE limit to it, do a PS integration and show the logs you get. Need the HE limit of PS integral from JA thesis and/or from VDD talk

Chapter 5

Z/γ^*+Jets at the LHC

5.1 Z+jets

Similarly to the the case of $W^{\pm}$ plus jets there are *four* possible emission sites for the boson; Two on the forward incoming quark, and two on the backward incoming quarks (see figure 5.1).

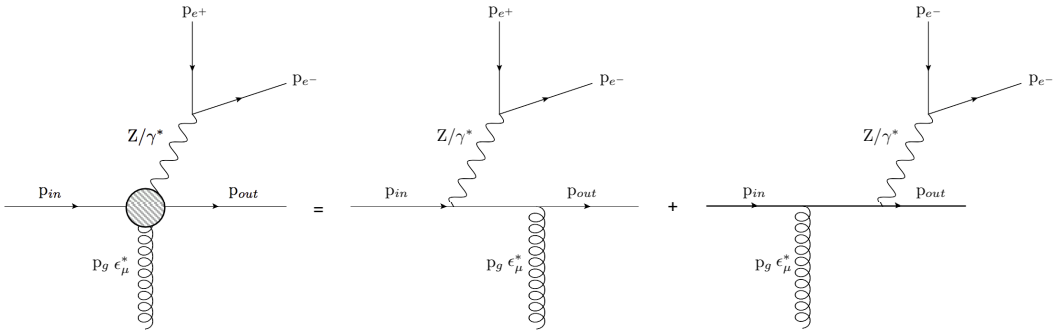

Figure 5.1: The possible emission sites for a neutral weak boson.

In the language of currents (see for *e.g.* [**?**]) we call the left hand side of figure 5.1 j_μ^{Z/γ^*}:

$$j_\mu^Z = \overline{u}^{h_{out}}(p_{out})\left(\gamma^\sigma \frac{\not{p}_{out}+\not{p}_Z}{(p_{out}+p_Z)^2}\gamma_\mu + \gamma_\mu \frac{\not{p}_{in}-\not{p}_Z}{(p_{in}-p_Z)^2}\gamma_\sigma\right) u^{h_{in}}(p_{in}) \times \overline{u}^{h_{e^-}}(p_{e^-})\gamma_\sigma u^{h_{e^+}}(p_{e^+}). \tag{5.1}$$

We can then express amplitudes in terms of contractions of 'emitting' and 'non-emitting' currents.

As the figure above indicates, when emitting a Z boson there is also the possiblity of an off-shell photon being exchanged instead of a Z. Since the difference in these two channels is indistinguishable in the final state we must treat the interference as the amplitude level. For example, the amplitude for $2 \to 2$ scattering is:

$$\mathcal{A}^{2\to 2}_{Z/\gamma^*} = \underbrace{\left(\frac{k_1}{p^2_{Z/\gamma^*} - m^2_Z + i\Gamma_Z m_Z} + \frac{Q_1 e}{p^2_{Z/\gamma^*}}\right)}_{\mathcal{K}_a} \frac{j_1^{Z/\gamma^*} \cdot j_2}{q^2_{t1}} + \underbrace{\left(\frac{k_2}{p^2_{Z/\gamma^*} - m^2_Z + i\Gamma_Z m_Z} + \frac{Q_2 e}{p^2_{Z/\gamma^*}}\right)}_{\mathcal{K}_b} \frac{j_1 \cdot j_2^{Z/\gamma^*}}{q^2_{b1}} \tag{5.2}$$

where k_i are the Z couplings to the quarks, Q_i are the the γ couplings to the quarks, m_Z is the mass of the Z, Γ_Z is the width of the Z peak, q_{t1} is the momentum of the t-channel gluon exchanged when Z emission occurs of the forward incoming quark line and q_{b1} is the momentum of the exchanged gluon when Z emission occurs of the backward incoming quark line.
Equation 5.2 is a good example of the advantages of using currents since the form of the diagrams for either Z or γ can be expressed as only two contraction (with the distinct propagators dealt with in the $\mathcal{K}_i$ terms).
Extra *real* gluon emissions from the t-channel gluon are then included using an effective vertex of the form [**?**][**?**]:

$$V^\rho(q_j, q_{j+1}) = -(q_j + q_{j+1})^\rho - 2\left(\frac{s_{aj}}{s_{ab}} - \frac{q^2_{j+1}}{s_{bj}}\right) p_b^\rho + 2\left(\frac{s_{bj}}{s_{ab}} + \frac{q^2_j}{s_{aj}}\right) p_a^\rho \tag{5.3}$$

Where $s_{aj} = 2p_a \cdot p_j$ *etc.* The general $2 \to n$ amplitude therefore looks like:

$$\begin{aligned}\mathcal{A}^{2\to n}_{Z/\gamma^*} = \Bigg(& \mathcal{K}_a \frac{V^{\mu_1}(q_{t1}, q_{t2}) \cdots V^{\mu_{n-2}}(q_{t(n-1)}, q_{t(n-2)})}{q_{t1} \cdots q_{t(n-1)}} j_1^Z \cdot j_2 + \ldots \\ & \mathcal{K}_b \frac{V^{\mu_1}(q_{b1}, q_{b2}) \cdots V^{\mu_{n-2}}(q_{b(n-1)}, q_{b(n-2)})}{q_{b1} \cdots q_{b(n-1)}} j_1 \cdot j_2^Z \Bigg) \epsilon^*_{\mu_1} \cdots \epsilon^*_{\mu_{(n-2)}}\end{aligned} \tag{5.4}$$

and after taking the modulus squared of this we have the following:

$$|\mathcal{A}^{2\to n}_{Z/\gamma^*}|^2 = \left|\mathcal{K}_a j_1^{Z/\gamma^*}\cdot j_2\right|^2 \frac{V^2(q_{t1},q_{t2})V^2(q_{t2},q_{t3})\cdots V^2(q_{b(n-2)},q_{b(n-1)})}{q^2_{t1}\cdots q^2_{t(n-1)}} + \ldots$$
$$\left|\mathcal{K}_b j_2^{Z/\gamma^*}\cdot j_1\right|^2 \frac{V^2(q_{b1},q_{b2})V^2(q_{b2},q_{b3})\cdots V^2(q_{b(n-2)},q_{b(n-1)})}{q^2_{b1}\cdots q^2_{b(n-1)}} + \ldots$$
$$2\Re\{\mathcal{K}_a\overline{\mathcal{K}_b}\times(j_1^{Z/\gamma^*}\cdot j_2)(\overline{j_2^{Z/\gamma^*}\cdot j_1})\}\frac{V(q_{t1},q_{t2})\cdot V(q_{b1},q_{b2})\cdots V(q_{t(n-2)},q_{t(n-1)})\cdot V(q_{b(n-2)},q_{b(n-1)})}{q_{t1}q_{b1}\cdots q_{t(n-1)}q_{b(n-1)}} \tag{5.5}$$

In previous work it was seen that the interference between forward quark- and backward weak boson emission (the third term in equation 5.5) was negligible [**?**]. This turns out not to be the case in Z plus jets - possibly due to the effects of photon interference.

5.1.1 Formulation in terms of currents

5.1.2 To High Multiplicity Final States

5.1.3 Emission-site Interference

5.1.4 Photonic Interference

5.1.5 The $2 \to n$ Matrix Element

5.1.6 The Fully Differential Z/γ^* Cross-Section

5.2 Regularising the Z/γ^*+Jets Matrix Element

Explain that in the MRK limit the external legs cant (by definition) be soft, then look at the limit of one gluon going soft (basically an NLO correction to the (n-1) parton ME) in the effective vertex. Show that this leads to a divergence.
Next talk about NLO virtual corrections to the (n-1)-parton ME. Show that in the HE limit, only two diagrams contribute (extra t - crosses and uncrossed - g exchange) show the log enhancement given. Give explicity calcultion showing divergences cancelling (as must happen by KLN theorem).

5.2.1 Soft Emissions

To calculate useful quantities such a cross sections *etc.* we must integrate equation 5.5 over all of phase space. However, problems arise when we attempt to integrate over the so called 'soft' (low energy) regions of phase space - things which should be finite diverge and need to be cancelled carefully. It is well understood that the divergences coming from soft *real* emissions cancel with those coming from soft *virtual* emissions and so we must explicitly show this cancellation and calculate the remaining finite contribution multiplying the $(n-1)$-final state parton matrix element.

In the previous work on $W^{\pm}$ emission the finite contribution was found to be [**?**][**?**]:

$$\frac{\alpha_s C_a \Delta_{j-1,j+1}}{\pi} \ln \frac{\lambda^2}{|\vec{q}_{j\perp}|^2}, \tag{5.6}$$

where α_s is the strong coupling strength, C_a is a numerical factor, $\Delta_{i-1,i+1}$ is the rapidity span of the final state partons either side of our soft emission, λ is a factor chosen to define the soft region: $p^2 < \lambda^2$ and $|\vec{q}_{j\perp}|^2$ is the sum of squares of the transverse components of the j^{th} t-channel gluon momenta.

Here we investigate the cancellation of these divergences for Z emission and most importantly whether the finite term is of the same form for the interference term which was previous disregarded.

We start by looking at a $2 \to n$ process and take the limit of one final state parton momentum, p_i, becoming small. Because of the form of equation 5.5 this ammounts to looking at the effect of soft-ness on equation 5.3, we can immediately see that for p_i going soft the gluon chain momenta coming into- and coming out of the j^{th} emission site will coincide: $q_{j+1} \sim q_j$:

$$V^{\rho}(q_j, q_{j+1}) \to -2q_j^{\rho} - 2\left(\frac{s_{aj}}{s_{ab}} - \frac{q_j^2}{s_{bj}}\right) p_b^{\rho} + 2\left(\frac{s_{bj}}{s_{ab}} + \frac{q_j^2}{s_{aj}}\right) p_a^{\rho} \tag{5.7}$$

In equation 5.5 we have two types of terms involving the effective vertex; Terms like $V^2(q_{t/bj}, q_{t/b(j+1)})$ and terms like $V(q_{tj}, q_{t(j+1)}) \cdot V(q_{bj}, q_{b(j+1)})$. The procedure for the V^2 terms doesnt not change between top-line emission and bottom-line emission and so only the calculation for top-line emission will be shown here.

5.2.2 $V^2(q_{tj}, q_{t(j+1)})$ Terms

Once we square equation 5.7 and impose on-shell conditions to p_a and p_b we get:

$$V^2(q_{tj}, q_{tj}) = 4q_j^2 + 8q_j{\cdot}p_b\left(\frac{s_{aj}}{s_{ab}} - \frac{q_j^2}{s_{bj}}\right) - 8q_j{\cdot}p_a\left(\frac{s_{bj}}{s_{ab}} + \frac{q_j^2}{s_{aj}}\right) - 4s_{ab}\left(\frac{s_{aj}}{s_{ab}} - \frac{q_j^2}{s_{bj}}\right)\left(\frac{s_{bj}}{s_{ab}} + \frac{q_j^2}{s_{aj}}\right) \tag{5.8}$$

Now since $p_j \to 0$ the terms s_{aj} and s_{bj} will also become vanishing:

$$V^2(q_{tj}, q_{tj}) = 4q_j^2 + 8q_j \cdot p_b\frac{q_j^2}{s_{bj}} - 8q_j \cdot p_a\frac{q_j^2}{s_{aj}} - 4s_{ab}\frac{q_j^4}{s_{bj}s_{aj}} \tag{5.9}$$

Clearly the final term now dominates due to its $\sim \frac{1}{p_i^2}$ behaviour:

$$V^2(q_{ti}, q_{ti}) = -\frac{4s_{ab}}{s_{bi}s_{ai}}q_i^4 + \mathcal{O}\left(\frac{1}{|p_i|}\right) \tag{5.10}$$

We must now explicitly calculate the invariant mass terms. Since we are in the high energy limit we may take $p_a \sim p_1 \sim p_+ = (\frac{1}{2}p_z, 0, 0, \frac{1}{2}p_z)$ and $p_b \sim p_n \sim p_- = (\frac{1}{2}p_z, 0, 0, -\frac{1}{2}p_z)$ and we describe our soft gluon by $p_i = (E, \vec{p})$. Therefore:

$$s_{ai} = 2p_a \cdot p_i \sim 2p_+ \cdot p_i = \frac{1}{2}p_z E - \frac{1}{2}p_z^2, \tag{5.11a}$$

$$s_{bi} = 2p_b \cdot p_i \sim 2p_- \cdot p_i = \frac{1}{2}p_z E + \frac{1}{2}p_z^2, \tag{5.11b}$$

and $s_{ab} = \frac{1}{2}p_z^2$. Then equation 5.10 reads:

$$V^2(q_{ti}, q_{ti}) = -\frac{4p_z^2}{(p_z E - p_z^2)(p_z E + p_z^2)}q_i^4 + \mathcal{O}\left(\frac{1}{|p_i|}\right), \tag{5.12a}$$

$$V^2(q_{ti}, q_{ti}) = -\frac{4p_z^2}{p_z^2(E^2 - p_z^2)}q_i^4 + \mathcal{O}\left(\frac{1}{|p_i|}\right), \tag{5.12b}$$

but since $E^2 - \vec{p}_1^2 = 0$:

$$V^2(q_{ti}, q_{ti}) = -\frac{4}{|\vec{p}_{1\perp}|^2}q_i^4 + \mathcal{O}\left(\frac{1}{|p_i|}\right), \tag{5.13}$$

Now looking back to equation 5.5 we see that each vertex is associated with factors of $(q_{ti}^{-2}q_{t(i+1)}^{-2})$ but once again since the emission is soft this becomes $(q_{ti}^{-4}$. This factor conspires to cancel with that in equation 5.13, moreover each vertex comes with a factor of $-C_A g_s^2$ (which are contained in the $\mathcal{K}_i$ terms in equation

5.5). Including these and dropping subdominant terms the final factor is:

$$\frac{4C_A g_s^2}{|\vec{p}_\perp|^2} \tag{5.14}$$

5.2.3 $V(q_{ti}, q_{t(i+1)}) \cdot V(q_{bi}, q_{b(i+1)})$ Terms

The calculation of the interference term with a soft emission follows similarly to the above section. After taking $p_i \to 0$ and dotting the two vertex terms together we have:

$$\begin{aligned} V(q_{ti}, q_{ti}) \cdot V(q_{bi}, q_{bi}) = 4q_i^t \cdot q_i^b - 4q_i^t \cdot p_a \left(\frac{s_{bi}}{s_{ab}} + \frac{t_i^b}{s_{ai}} \right) + 4q_i^t \cdot p_b \left(\frac{s_{ai}}{s_{ab}} + \frac{t_i^b}{s_{bi}} \right) \dots \\ - 4q_i^b \cdot p_a \left(\frac{s_{bi}}{s_{ab}} + \frac{t_i^t}{s_{ai}} \right) + 4q_i^b \cdot p_b \left(\frac{s_{ai}}{s_{ab}} + \frac{t_i^t}{s_{bi}} \right) \dots \end{aligned} \tag{5.15}$$

having use $p_a^2 = 0$ and $p_b^2 = 0$ once again. We can drop all the terms with s_{ai} or s_{bi} in the denominator and this time we are left with *two* dominant terms which combine to give:

$$V(q_{ti}, q_{ti}) \cdot V(q_{bi}, q_{bi}) = -\frac{s_{ab}}{s_{ai} s_{bi}} t_i^t t_i^b + \mathcal{O}\left(\frac{1}{|p_i|} \right). \tag{5.16}$$

The invariant mass terms here are identical to those we say in the V^2 terms and the products of $t_i^t t_i^b$ also appear in the denominator of the interference term in equation 5.5. After this cancelling we are left with exactly what we had before (see equation 5.14).

Since exactly the same factor comes from all three terms at the amplitude squared level we may factor them out and express the amplitude squared for an n-parton final state with one soft emission in terms of an $(n-1)$-parton final state amplitude squared multiplied by our factor:

$$\lim_{p_i \to 0} |\mathcal{A}_{Z/\gamma^*}^{2 \to n}|^2 = \left(\frac{4C_A g_s^2}{|\vec{p}_{i\perp}|^2} \right) |\mathcal{A}_{Z/\gamma^*}^{2 \to (n-1)}|^2 \tag{5.17}$$

5.2.4 Integration of soft diverences

As mentioned above the divergences only become apparent after we have attempted to integrate over phase space. The Lorentz invariant phase space integral associated with p_i is:

$$\int \frac{d^3\vec{p}_i}{(2\pi)^3 2E_i} \frac{4C_A g_s^2}{|\vec{p}_\perp|^2}. \tag{5.18}$$

It is convenient to replace the integral over the z-component of momentum with one over rapidity, y_2. Rapidty and momentum are realted through:

$$y = \frac{1}{2} \ln \left(\frac{E + p_z}{E - p_z} \right) \tag{5.19}$$

The Jacobian of this transformation is:

$$\frac{dy}{dp_z} = \frac{1}{2(E+p_z)} \frac{\partial}{\partial p_z}(E + p_z) - \frac{1}{2(E-p_z)} \frac{\partial}{\partial p_z}(E - p_z), \tag{5.20}$$

$$= \frac{E}{E^2 - p_z^2} - \frac{p_z}{E^2 - p_z^2} \frac{\partial E}{\partial p_z}, \tag{5.21}$$

$$= \frac{E}{E^2 - p_z^2} - \frac{p_z}{E^2 - p_z^2} \frac{p_z}{E}, \tag{5.22}$$

$$= \frac{1}{E}. \tag{5.23}$$

The phase space integral then reads:

$$\int \frac{d^{2+2\epsilon}\vec{p}_\perp}{(2\pi)^{2+2\epsilon}} \frac{dy}{4\pi} \frac{4C_A g_s^2}{|\vec{p}_\perp|^2} \mu^{-2\epsilon} = \frac{4C_A g_s^2 \mu^{-2\epsilon}}{(2\pi)^{2+2\epsilon} 4\pi} \Delta_{i-1,i+1} \int \frac{d^{2+2\epsilon}\vec{p}_\perp}{|\vec{p}_\perp|^2}, \tag{5.24}$$

where we have analytically continued the integral to $2+2\epsilon$ dimensions to regulate the divergence and introduced the parameter μ to keep the coupling dimensionless in the process. Converting to polar cooerdinates and using the result for the volume of a unit hypersphere gives to integrated soft contribution:

$$\frac{4C_A g_s^2}{(2\pi)^{2+2\epsilon} 4\pi} \Delta_{i-1,i+1} \frac{1}{\epsilon} \frac{\pi^{1+\epsilon}}{\Gamma(\epsilon + 1)} \left(\frac{\lambda^2}{\mu^2} \right)^\epsilon \tag{5.25}$$

5.2.5 Virtual Emissions

The virtual emission diagrams are included using the Lipatov ansatz for the gluon propagator:

$$\frac{1}{q_i^2} \longrightarrow \frac{1}{q_i^2} e^{\hat{\alpha}(q_i)(\Delta_{i,i-1})}, \tag{5.26}$$

where:

$$\hat{\alpha}(q_i) = \alpha_s C_A q_i^2 \int \frac{d^{2+2\epsilon}k_\perp}{(2\pi)^{2+2\epsilon}} \frac{1}{k_\perp^2 (k_\perp - q_{i\perp})^2} \mu^{-2\epsilon}. \tag{5.27}$$

Once again we choose to perform the integral using dimensional regularistion. Using the well known Feynman parameterisation formulae gvies:

$$\hat{\alpha}(q_i) = \alpha_s C_A q_i^2 \int \frac{d^{2+2\epsilon}k_\perp}{(2\pi)^{2+2\epsilon}} \int_0^1 \frac{dx}{[x(k-q_i)_\perp^2 + (1-x)k_\perp^2]^2} \mu^{-2\epsilon}, \tag{5.28}$$

$$= \alpha_s C_A q_i^2 \int \frac{d^{2+2\epsilon}\hat{k}_\perp}{(2\pi)^{2+2\epsilon}} \int_0^1 \frac{dx}{[\hat{k}_\perp^2 + q_{i\perp}^2(1-x)]^2} \mu^{-2\epsilon}, \tag{5.29}$$

where we have performed a change of variables to $\hat{k}_\perp = k_\perp - x q_{i\perp}$ with unit Jacobian. Changing the order of integration we can perform the $\hat{k}_\perp$ integral using the following result:

$$\int \frac{d^d k}{(2\pi)^d} \frac{1}{(k^2 - C)^\alpha} = \frac{1}{(4\pi)^{\frac{d}{2}}} \frac{\Gamma(\alpha - \frac{d}{2})}{\Gamma(\alpha)} \frac{(-1)^\alpha}{C^{\alpha - \frac{d}{2}}}, \tag{5.30}$$

to give:

$$\hat{\alpha}(q_i) = \alpha_s C_A q_i^2 \frac{\Gamma(1-\epsilon)}{(4\pi)^{1+\epsilon}} (-q_{i\perp}^2)^{\epsilon-1} \int_0^1 dx (1-x)^{\epsilon-1}, \tag{5.31}$$

$$= -\frac{2 g_s^2 C_A}{(4\pi)^{2+\epsilon}} \frac{\Gamma(1-\epsilon)}{\epsilon} \left(\frac{q_{i\perp}^2}{\mu^2}\right)^\epsilon, \tag{5.32}$$

having completed the x integral and used $\alpha_s = \frac{g_s^2}{4\pi}$.

5.2.6 Cancellation of Infrared Contributions

We now show how the infrared contributions from soft real emissions and virtual emissions cancel leaving our integrated matrix element finite. The subtlety here is that we must sum two diagrams with different final states to see the cancellation. This is because they are experimentally indistinguishable; The $2 \to (n-1)$ virtual diagram has $(n-1)$ resolvable partons in the final state (but is a higher order diagram perturbatively speaking). Because on of the emission in the real $2 \to n$ diagram is soft it is experimentally undetectable so we detect the same final state as the virtual diagram.
The matrix element squared for the real soft diagram will look like:

$$|\mathcal{A}^{2\to n}_{Z/\gamma^*}|^2 = \left(\frac{4g_s^2 C_a}{|p_{i\perp}|^2}\right)\Bigg[\left|\mathcal{K}_a j_1^{Z/\gamma^*}\cdot j_2\right|^2 \frac{\prod_{i\neq j}^{n-2} V^2(q_{ti}, q_{t(i+1)})}{\prod_{i\neq j}^{n-1} q_{ti}^2} + \ldots \tag{5.33}$$

$$\left|\mathcal{K}_b j_2^{Z/\gamma^*}\cdot j_1\right|^2 \frac{\prod_{i\neq j}^{n-2} V^2(q_{bi}, q_{b(i+1)})}{\prod_{i\neq j}^{n-1} q_{bi}^2} + \ldots \tag{5.34}$$

$$2\Re\{\mathcal{K}_a\overline{\mathcal{K}_b}\times(j_1^{Z/\gamma^*}\cdot j_2)(\overline{j_2^{Z/\gamma^*}\cdot j_1})\}\frac{\prod_{i\neq j}^{n-2} V(q_{ti}, q_{t(i+1)})\cdot V(q_{bi}, q_{b(i+1)}))}{\prod_{i\neq j}^{n-1} q_{ti}q_{bi}}\Bigg], \tag{5.35}$$

where we have taken the i^{th} gluon to be soft and the result of the Lorentz invariant phase space integration over the p_i momentum is shown in equation 5.25.
After inserting the Lipatov ansatz into the $2 \to (n-1)$ matrix element squared we have:

$$|\mathcal{A}^{2\to(n-1)}_{Z/\gamma^*}|^2 = \left|\mathcal{K}_a j_1^{Z/\gamma^*}\cdot j_2\right|^2 \frac{\prod_{i}^{n-3} V^2(q_{ti}, q_{t(i+1)})}{\prod_{i}^{n-2} q_{ti}^2} e^{2\hat{\alpha}(q_{ti})\Delta_{i-1,i+1}} + \ldots \tag{5.36}$$

$$\left|\mathcal{K}_b j_2^{Z/\gamma^*}\cdot j_1\right|^2 \frac{\prod_{i}^{n-3} V^2(q_{bi}, q_{b(i+1)})}{\prod_{i}^{n-2} q_{bi}^2} e^{2\hat{\alpha}(q_{bi})\Delta_{i-1,i+1}} + \ldots \tag{5.37}$$

$$2\Re\{\mathcal{K}_a\overline{\mathcal{K}_b}\times(j_1^{Z/\gamma^*}\cdot j_2)(\overline{j_2^{Z/\gamma^*}\cdot j_1})\}\frac{\prod_{i}^{n-3} V(q_{ti}, q_{t(i+1)})\cdot V(q_{bi}, q_{b(i+1)}))}{\prod_{i}^{n-2} q_{ti}q_{bi}} e^{(\hat{\alpha}(q_{bi})+\hat{\alpha}(q_{bi}))\Delta} \tag{5.38}$$

We can now go through term-by-term to show the divergences cancel and find

the finite contribution to the matrix element squared. Similarly to when we calculated the soft terms the pure top and bottom emissions follow identically so here we will only state the procedure for the top emission. The interference term is slightly different.

For the top line emission we have the following terms:

$$\frac{4C_A g_s^2}{(2\pi)^{2+2\epsilon}4\pi}\Delta_{i-1,i+1}\frac{1}{\epsilon}\frac{\pi^{1+\epsilon}}{\Gamma(\epsilon+1)}\left(\frac{\lambda^2}{\mu^2}\right)^{\epsilon} + e^{2\hat{\alpha_s}(q_{ti})\Delta_{i-1,i+1}}. \tag{5.39}$$

We now extract the relevant term (in terms of the strong coupling order) from the exponential and substitute the expression for $\hat{\alpha_s}$:

$$= \frac{4C_A g_s^2}{(2\pi)^{2+2\epsilon}4\pi}\Delta_{i-1,i+1}\frac{1}{\epsilon}\frac{\pi^{1+\epsilon}}{\Gamma(\epsilon+1)}\left(\frac{\lambda^2}{\mu^2}\right)^{\epsilon} - -\frac{2g_s^2 C_A}{(4\pi)^{2+\epsilon}}\frac{\Gamma(1-\epsilon)}{\epsilon}\left(\frac{q_{ti\perp}^2}{\mu^2}\right)^{\epsilon}, \tag{5.40}$$

$$= \frac{g_s^2 C_A}{4^{1+\epsilon}\pi^{2+\epsilon}}\Delta_{i-1,i+1}\left(\frac{1}{\epsilon\Gamma(1+\epsilon)}\left(\frac{\lambda^2}{\mu^2}\right)^{\epsilon} - \frac{\Gamma(1-\epsilon)}{\epsilon}\left(\frac{q_{ti\perp}^2}{\mu^2}\right)^{\epsilon}\right). \tag{5.41}$$

Expanding the terms involving ϵ yeilds:

$$\frac{1}{\Gamma(1+\epsilon)} = 1 + \gamma_E\epsilon + \mathcal{O}(\epsilon^2), \tag{5.42a}$$

$$\Gamma(1-\epsilon) = 1 + \gamma_E\epsilon + \mathcal{O}(\epsilon^2), \tag{5.42b}$$

$$\left(\frac{x}{y}\right)^{\epsilon} = 1 + \epsilon\ln\left(\frac{x}{y}\right) + \mathcal{O}(\epsilon^2). \tag{5.42c}$$

And so the finite terms are:

$$= \frac{g_s^2 C_A\Delta_{i-1,i+1}}{4^{1+\epsilon}\pi^{2+\epsilon}}\left((1+\gamma_E\epsilon+\mathcal{O}(\epsilon^2))\left(\frac{1}{\epsilon}+\ln\left(\frac{\lambda^2}{\mu^2}\right)+\mathcal{O}(\epsilon)\right) - (1+\gamma_E\epsilon+\mathcal{O}(\epsilon^2))\left(\frac{1}{\epsilon}+\ln\left(\frac{q_{ti\perp}^2}{\mu^2}\right.\right.\right. \tag{5.43a}$$

$$= \frac{g_s^2 C_A\Delta_{i-1,i+1}}{4\pi^2}\ln\left(\frac{\lambda^2}{q_{ti\perp}^2}\right) \tag{5.43b}$$

$$= \frac{\alpha_s C_A\Delta_{i-1,i+1}}{\pi}\ln\left(\frac{\lambda^2}{q_{ti\perp}^2}\right) \tag{5.43c}$$

Likewise for the emission purely from the backward quark line we have:

$$= \frac{\alpha_s C_A\Delta_{i-1,i+1}}{\pi}\ln\left(\frac{\lambda^2}{q_{bi\perp}^2}\right) \tag{5.44}$$

For the interference we expand the exponential with both forward emission q momenta and backward emission q momenta to get:

$$= \frac{g_s^2 C_A \Delta_{i-1,i+1}}{4^{1+\epsilon}\pi^{2+\epsilon}} \left(\left(\frac{1}{\epsilon} + \gamma_E + \ln\left(\frac{\lambda^2}{\mu^2}\right) + \mathcal{O}(\epsilon) \right) - \frac{1}{2}\left[\frac{2}{\epsilon} + 2\gamma_E + \ln\left(\frac{q_{ti\perp}^2}{\mu^2}\right) - \ln\left(\frac{q_{bi\perp}^2}{\mu^2}\right) + \mathcal{O}(\epsilon) \right. \right. \tag{5.45a}$$

$$= \frac{\alpha_s C_A \Delta_{i-1,i+1}}{\pi} \ln\left(\frac{\lambda^2}{\sqrt{q_{ti\perp}^2 q_{bi\perp}^2}}\right) \tag{5.45b}$$

This is a very similar form to that found in [**?**] and [**?**].

5.3 Example: $2 \to 4$ Scattering

As an example we show the cancellation explicitly for the case of $2 \to 4$ when the p_2 momentum has gone soft. A contributing soft diagram is shown in figure 5.2 and one example of a contributing virtual diagram of the same order is shown in figure 5.3. When p_2 goes soft we have the following form for the $2 \to 4$ integrated amplitude squared (N.B.: The integration is only schematic and doesnt represent the full Lorentz invariant phase space):

$$\begin{aligned}\int |\mathcal{A}_{soft}^{2\to 4}|^2 =& \frac{4C_A g_s^2 \Delta_{1,3}}{(2\pi)^{2+2\epsilon} 4\pi} \frac{\pi^{\epsilon+1}}{\epsilon\Gamma(\epsilon+1)} \left(\frac{\lambda^2}{\mu^2}\right)^{\epsilon} \left[|\mathcal{K}_a j_1^Z \cdot j_2|^2 \frac{V^2(q_{t1}, q_{t3})}{q_{t1}^2 q_{t3}^2} + |\mathcal{K}_b j_1 \cdot j_2^Z|^2 \frac{V^2(q_{b1}, q_{b3})}{q_{b1}^2 q_{b3}^2} + \dots \right. \\ & \left. 2\Re\left\{ \mathcal{K}_a \overline{\mathcal{K}_b} (j_1^Z \cdot j_2) \overline{(j_1 \cdot j_2^Z)} \right\} \frac{V(q_{t1}, q_{t3}) \cdot V(q_{b1}, q_{b3})}{q_{t1} q_{t3} q_{b1} q_{b3}} \right],\end{aligned} \tag{5.46}$$

and the virtual contributions for the $2 \to 3$ amplitude is:

$$\begin{aligned}\int |\mathcal{A}_{virtual}^{2\to 3}|^2 =& |\mathcal{K}_b j_1 \cdot j_2^Z|^2 \frac{V^2(q_{t1}, q_{t3})}{q_{t1}^2} e^{2\hat{\alpha}(q_{t1})\Delta_{1,3}} + |\mathcal{K}_t j_1^Z \cdot j_2|^2 \frac{V^2(q_{b1}, q_{b3})}{q_{b1}^2} e^{2\hat{\alpha}(q_{b1})\Delta_{1,3}} + \dots \\ & 2\Re\left\{ \mathcal{K}_a \overline{\mathcal{K}_b} (j_1^Z \cdot j_2) \overline{(j_1 \cdot j_2^Z)} \right\} \frac{V(q_{t1}, q_{t3}) \cdot V(q_{b1}, q_{b3})}{q_{t1} q_{t3} q_{b1} q_{b3}} e^{(\hat{\alpha}(q_{t1}) + \hat{\alpha}(q_{b1}))\Delta_{1,3}}.\end{aligned} \tag{5.47}$$

Once we expand the exponential to the correct order in g_s^2, the sum of these

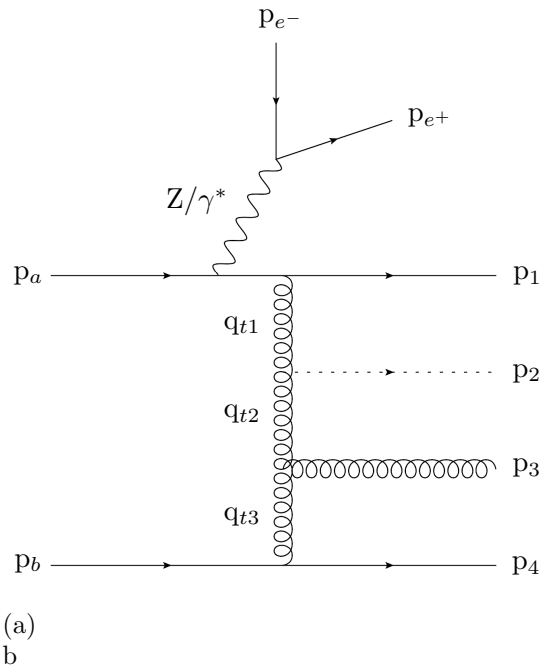

Figure 5.2: Soft Emission

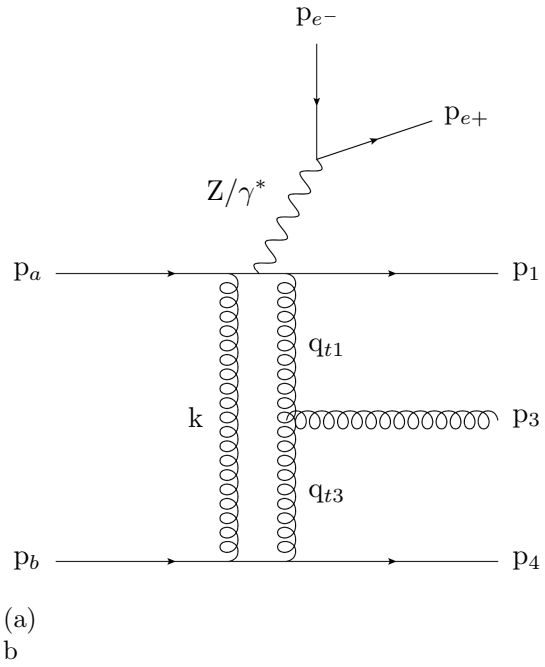

Figure 5.3: Virtual Emission

Figure 5.4: Examples of diagrams contributing to $2 \to 4$ scattering. In figure 5.2 the p_2 has been drawn with a dashed line to denote it is not resolvable. In figure 5.3 the final state momenta have been labelled in a seemingly strange way - this was done to make clear the cancellation when working through the algebra.

matrix elements squared over the region of phase space when p_2 is soft is:

$$\begin{aligned}\int \left(|\mathcal{A}^{2\to4}_{soft}|^2 + |\mathcal{A}^{2\to3}_{virtual}|^2\right) =& |\mathcal{K}_a j_1^Z \cdot j_2|^2 \frac{V^2(q_{t1}, q_{t3})}{q_{t1}^2}\left(\frac{4C_A g_s^2 \Delta_{1,3}}{(2\pi)^{2+2\epsilon}4\pi}\frac{\pi^{\epsilon+1}}{\epsilon\Gamma(\epsilon+1)} - 2\hat{\alpha}(q_{t1})\Delta_{1,3}\right) + \dots \\ & |\mathcal{K}_b j_1 \cdot j_2^Z|^2 \frac{V^2(q_{b1}, q_{b3})}{q_{b1}^2}\left(\frac{4C_A g_s^2 \Delta_{1,3}}{(2\pi)^{2+2\epsilon}4\pi}\frac{\pi^{\epsilon+1}}{\epsilon\Gamma(\epsilon+1)} - 2\hat{\alpha}(q_{b1})\Delta_{1,3}\right) + \dots \\ 2\Re\left\{\mathcal{K}_a\overline{\mathcal{K}_b}(j_1^Z \cdot j_2)\overline{(j_1 \cdot j_2^Z)}\right\} & \frac{V(q_{t1}, q_{t3}) \cdot V(q_{b1}, q_{b3})}{q_{t1}q_{t3}q_{b1}q_{b3}}\left(\frac{4C_A g_s^2 \Delta_{1,3}}{(2\pi)^{2+2\epsilon}4\pi}\frac{\pi^{\epsilon+1}}{\epsilon\Gamma(\epsilon+1)} - (\hat{\alpha}(q_{t1}) + \hat{\alpha}(q_{b1}))\Delta_{1,3}\right.\end{aligned} \tag{5.48}$$

These bracketed terms are exactly the cancellations calculated in section 4 above. Therefore:

$$\begin{aligned}\int \left(|\mathcal{A}^{2\to4}_{soft}|^2 + |\mathcal{A}^{2\to3}_{virtual}|^2\right) = \frac{\alpha_s C_A \Delta_{1,3}}{\pi}\Bigg(& |\mathcal{K}_a j_1^Z \cdot j_2|^2 \frac{V^2(q_{t1}, q_{t3})}{q_{t1}^2}\ln\left(\frac{\lambda^2}{|q_{1t\perp}|^2}\right) + \dots \\ & |\mathcal{K}_b j_1 \cdot j_2^Z|^2 \frac{V^2(q_{b1}, q_{b3})}{q_{b1}^2}\ln\left(\frac{\lambda^2}{|q_{1b\perp}|^2}\right) + \dots \\ & 2\Re\left\{\mathcal{K}_a\overline{\mathcal{K}_b}(j_1^Z \cdot j_2)\overline{(j_1 \cdot j_2^Z)}\right\}\frac{V(q_{t1}, q_{t3}) \cdot V(q_{b1}, q_{b3})}{q_{t1}q_{t3}q_{b1}q_{b3}}\ln\left(\frac{\lambda^2}{\sqrt{|q_{1t\perp}|^2|q_{1b\perp}|^2}}\right)\Bigg) + \mathcal{O}(\alpha_s^2),\end{aligned} \tag{5.49}$$

Which is manifestly finite.

Chapter 6

$t\bar{t}$+Jets in the High Energy Limit

Chapter 7

Experimental Comparison

7.1 High multiplicity jets at ATLAS

7.2 The $W^{\pm}$ to Z/γ^{*} ratio at ATLAS

Chapter 8

Conclusions and Outlook

Publications

Author Name(s). Title of publication. In *Where Published*, Year.

Author Name(s). Title of publication. In *Where Published*, Year.